Earth Planet. Sci. Lett. 678 (2026) 119847

Contents lists available at ScienceDirect

Earth and Planetary Science Letters

journal homepage: www.elsevier.com/locate/epsl

Limited crustal contamination in large igneous province basalts: Sr-Nd-Pb-Os isotope evidence from the Western Ghats, Deccan Traps

A. Marzoli [a,*], L. Reisberg [b], M. Capriolo [c], S. Callegaro [d], P.R. Renne [e,f], M. Chiaradia [g], C.M. Meyzen [h], S. Self [f], L. Vanderkluysen [i], A. Boscaini [j]

[a] Dipartimento del Territorio e Sistemi Agro-Forestali, Università di Padova, Italy
[b] Centre de Recherches Pétrographiques et Géochimiques, CNRS-University of Lorraine, Nancy, France
[c] School of Geography, Earth and Environmental Sciences, University of Birmingham, United Kingdom
[d] Department of Biological Geological and Environmental Sciences, University of Bologna, Italy
[e] Berkeley Geochronology Center, Berkeley, USA
[f] Department of Earth and Planetary Science, University of California, Berkeley, USA
[g] Department of Earth Sciences, University of Geneva, Switzerland
[h] Dipartimento di Geoscienze, Università di Padova, Italy
[i] Department of Biodiversity, Earth and Environmental Science, Drexel University, Philadelphia, USA
[j] Département des Sciences de la Terre et de l'Atmosphère/Geotop, Université du Québec à Montréal, 201, avenue du Président-Kennedy, Montréal, Québec H2X 3Y7, Canada

ARTICLE INFO

Editor: Dr C. M. Petrone

Keywords:
Basalt
Deccan
Large igneous province
Crustal assimilation
Mantle source

ABSTRACT

The origin of basalts from the Western Ghats lava sequences of the Deccan large igneous province (LIP) was investigated through combined major and trace element and isotopic analysis. Sr-Nd-Pb isotopic compositions are strongly variable and show a time-related shift from enriched, crustal-like values for the late Cretaceous Kalsubai and Lonavala Subgroup basalts to more depleted mantle-like values for the early Paleogene Wai Subgroup basalts. By contrast, Os isotopic data are relatively uniform from base to top of the Western Ghats (initial $^{187}Os/^{188}Os_i$ at 66 Ma: 0.12-0.21) and generally similar to those of the present-day Réunion mantle plume. The basalts from the Wai Subgroup Ambenali Formation ($^{187}Os/^{188}Os_i$ 0.120) may show a moderate contribution from the sub-continental lithospheric mantle. In general, the combined isotopic and trace element compositions, and $^{187}Os/^{188}Os_i$ in particular, show that assimilation of the Proterozoic to Archean Indian crust was generally low (<3 wt.% of starting magma) and did not exceed 8 wt.% in any of the studied lavas. Similar results have been previously reported for other Phanerozoic LIPs. Therefore, we suggest that the emplacement of LIPs as short-lived eruptive pulses interrupted by relatively longer hiatus periods possibly hindered effective and prolonged heating of the basement rocks above their solidus temperature. Most likely, this obstacle to crustal contamination was particularly effective for the Wai basalts, which are interlayered with numerous sedimentary or paleosol layers probably formed during periods of volcanic quiescence when the crustal basement may have returned to low sub-solidus temperatures.

1. Introduction

Compared to basaltic magmas generated in the shallow convecting mantle (e.g., Mid-Ocean Ridge Basalts, MORB) those from large igneous provinces (LIPs) generally have higher incompatible trace element contents and radiogenic isotope compositions (Mahoney et al., 1982) indicating long-term incompatible element enrichment (hereafter "enriched compositions"). This enrichment may be due to the presence of recycled crustal components in the mantle source (e.g., Melluso et al., 2006), or to interaction of the magmas with the continental lithospheric mantle (SCLM) and crust (e.g., Peng et al., 1994; Reisberg and Aulbach, 2025).

The Archean to Proterozoic age and thus strongly enriched isotopic compositions of the Indian basement rocks makes the 66 Ma Deccan Province an ideal site to assess the amounts of crustal contamination in continental LIPs. The Re-Os isotopic system, especially when used

* Corresponding author.
E-mail address: andrea.marzoli@unipd.it (A. Marzoli).

https://doi.org/10.1016/j.epsl.2026.119847
Received 22 June 2025; Received in revised form 5 January 2026; Accepted 9 January 2026
0012-821X/© 2026 Elsevier B.V. All rights are reserved, including those for text and data mining, AI training, and similar technologies.

alongside traditional isotopic tracers (Sr, Nd, Pb), offers a powerful tool for detecting the potential contribution of assimilated continental lithospheric components. This is due to the markedly distinct Os isotope signatures of continental crust, sub-continental lithospheric mantle (SCLM), and convecting mantle. These strong differences arise from the fact that, unlike the other commonly used radiogenic tracers, Os behaves compatibly during partial melting of the mantle while its parent, Re, is mildly incompatible. As a result, the crust has low Os concentrations and very high Re/Os ratios (Saal et al., 1998; Peucker-Ehrenbrink and Jahn, 2001), which evolve with time into very high $^{187}Os/^{188}Os$ ratios. By contrast, the SCLM has low $^{187}Os/^{188}Os$ ratios, coupled with high Os concentrations (e.g., Carlson, 2005; Aulbach et al., 2016), making these Os isotopic ratios largely resistant to disturbance by the metasomatic agents that often perturb the Sr, Nd and Pb isotope systematics of this domain. The $^{187}Os/^{188}Os$ ratios of magmas from the convecting mantle or mantle plumes are much lower than those of crustal rocks, but typically higher than those of the SCLM, particularly the cratonic SCLM (e.g., Gannoun et al., 2016).

We combine new $^{187}Os/^{188}Os$ data with major and trace element compositions and Sr, Nd and Pb isotope data on selected basaltic samples that are stratigraphically well-positioned to constrain the extent and time-related evolution of lithospheric mantle and crustal contribution for the Western Ghats (WG) volcanic pile of the Deccan LIP. Detailed geochronologic and volcanostratigraphic data (e.g., Beane et al., 1986; Schoene et al., 2019; Sprain et al., 2019) allow the studied samples to be assigned to the different volcanic formations of the WG. We show that the calculated degrees of crustal assimilation are generally moderate to very low even for the WG basalts with the most enriched Sr, Nd and Pb isotopic compositions. As similar conclusions apply to basaltic magmas from other continental LIPs, we propose an interpretation of the crustal contamination process in LIPs grounded in recent concepts regarding the evolution of their transcrustal plumbing systems (Mittal et al., 2021).

2. The Deccan

The volumetrically dominant exposed portion of the Deccan Traps (Fig. 1) was emplaced between ca. 66.8 and 65.4 Ma (e.g., Schoene et al., 2019; Sprain et al., 2019; Tholt et al., 2023), straddling the Cretaceous-Paleogene boundary (*ca.* 66.0 Ma; Sprain et al., 2018) and arguably contributing to the end-Cretaceous extinction event (e.g., Callegaro et al., 2023). Since the work of Morgan (1972), the formation of this LIP is commonly attributed to the Réunion mantle plume, which impinged on the rapidly northward migrating Indian continental plate (but see alternative interpretations, e.g., in Sheth, 2007). The Western Ghats (WG) section in the Main Deccan (Fig. 1) yielded $^{40}Ar/^{39}Ar$ dates from lavas and U-Pb dates from zircons in paleosol or sedimentary interbeds ranging from ca. 66.3 to 65.5 Ma (Schoene et al., 2019; Sprain et al., 2019). On the WG escarpment east of Mumbai, central-western India, more than 3000 m of composite volcanic stratigraphy are exposed (Beane et al., 1986). Based on field evidence and geochemical compositions (in particular, Sr, Nd, Pb isotopic ratios), the WG lavas have been subdivided into 3 subgroups (from base to top: Kalsubai, Lonavala, Wai) and 11 lava flow formations (Fig. 1b; e.g., Beane et al., 1986; Kale et al., 2019). Dykes with geochemical affinity to the Kalsubai and Lonavala flows are dominant in the Narmada-Tapi graben, while Wai lava flows are geochemically similar to Central Deccan dykes and to dykes intruded along the coast of the Arabian Sea (Vanderkluysen et al., 2011; Fig. 1). Scarce $^{187}Os/^{188}Os$ data from previous studies on the WG (Allègre et al., 1999; Peters et al., 2017; Peters and Day, 2017) were in part obtained on mafic samples of poorly constrained volcanostratigraphic position and are generally not combined with Sr, Nd, Pb isotopic data.

3. Methods

Details on all the analytical methods are reported in the

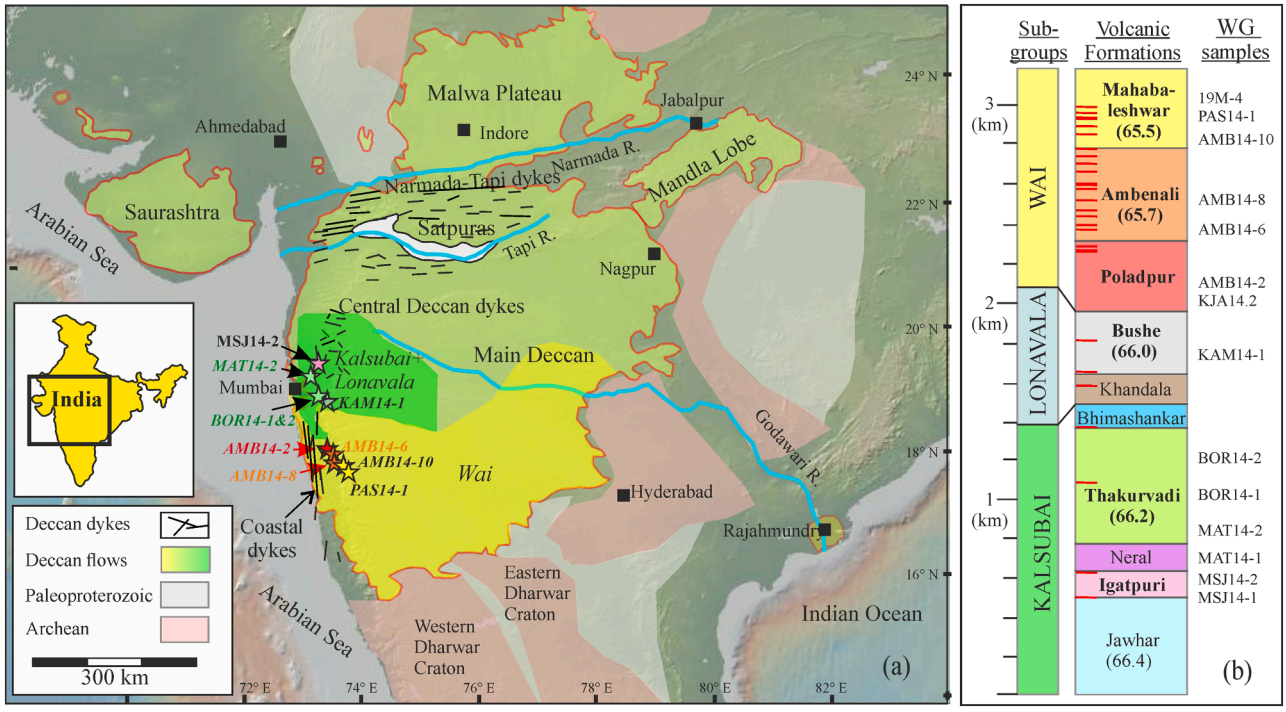

Fig. 1. **a**: Schematic geological map of the Deccan LIP and of the surrounding Indian cratons (Archean rocks and inter-cratonic Paleoproterozoic suture zones; modified after Self et al., 2022). Location of the Kalsubai plus Lonavala (bright green field) and Wai basalts (yellowish-greenish field) as well as main dyke swarms (black lines; cf. Vanderkluysen et al., 2011) are schematically shown after Self et al. (2022). Sampling locations for rocks analyzed here for Re-Os are marked with stars. **1b**: volcanic stratigraphy of Western Ghats lava flow subgroups and formations (after Sprain et al., 2019) with interlayered red boles (i.e., soil and/or sedimentary horizons, shown by red lines) and approximate stratigraphic positions of the analyzed basaltic rock samples (the low-volume Panhala Formation above Mahabaleshwar Fm. is not shown). Numbers in brackets indicate the approximate age in Ma for the main formations based on data from Sprain et al. (2019).

Supplementary Information. Whole-rock major and trace elements were analyzed on powdered whole-rock samples by X-ray fluorescence at Padova University (Italy) and by Inductively Coupled Plasma-Mass Spectrometry (ICP-MS) at Université de Bretagne Occidentale, Brest (France), following procedures described in the Supplementary Information. Radiogenic isotope ratios of Sr, Nd, and Pb were measured on a Multicollector ICP-MS at the Department of Earth Sciences (University of Geneva, Switzerland; Chiaradia et al., 2020).

Rhenium-osmium analyses were performed at the Centre de Recherches Pétrographiques et Géochimiques (CRPG-CNRS; University of Lorraine) in Nancy (France). After chemical separation, Os isotope compositions were analyzed by negative thermal ionization mass spectrometry (Creaser et al., 1991; Völkening et al., 1991) using either a Finnigan MAT262 or a ThermoScientific Triton instrument. Re isotope compositions for isotope dilution concentration calculations were measured using a ThermoScientific Neptune MC-ICPMS.

4. Results

4.1. Major and trace elements

We report geochemical results for 14 samples from the Western Ghats (Table 1 and Supplementary Information Table S1), comprising rocks from the three subgroups (Kalsubai, Lonavala, Wai; see Fig. 1b for sample positions in the stratigraphic column). All have been analyzed for major and trace elements and Sr, Nd, Pb isotopic compositions. For 10 of these samples, we obtained Re-Os isotopic compositions (Table 1).

All the analyzed rocks fall within the major and trace element fields of previously published WG lavas (thin section images, classification and major element diagrams are in the Supplementary Information, Figs. S1–S3). Except for two basaltic andesites from the Thakurvadi Formation (BOR14-1 and BOR14-2; SiO_2 52.0-52.3 wt.%) they can be classified as basalts (SiO_2 48.2-51.2 wt.%). In agreement with previous studies (Beane et al., 1986), the MgO contents of WG lavas are generally low (8.2-4.5 wt.%) except for one basaltic andesite (BOR14-2; MgO 13.5 wt.%). This latter sample has an unusual geochemical composition and a coarse grained texture indicating that it does not represent a magmatic liquid composition (for further details on this sample see the Supplementary Information). As known from previous studies, Wai Subgroup basalts tend in general to be relatively low in SiO_2 and K_2O (<0.6 wt.%) and high in TiO_2 (>2.1 wt.%) when compared to Kalsubai and in particular to Lonavala samples, which comprise low-Ti (TiO_2 < 2.0 wt.%) and high-Ti (TiO_2 > 2.0 wt.%) basalts. Apart from one sample (again, BOR14-2), Loss On Ignition (LOI) of all the analyzed samples is lower than 2.4 wt.%, suggesting that they are not significantly altered (*cf.* thin section images and petrographic descriptions in the Supplementary Information).

Trace element contents and ratios (Fig. 2) vary substantially among the 11 Formations from the WG and occasionally even within single formations (e.g., Thakurvadi, present and literature data, e.g., Basu et al., 2020). This has been interpreted as evidence for the involvement of distinct parental magmas and possibly of variable mantle and crustal contributions to WG basalts (e.g., Peng et al., 1994; Basu et al., 2020; Pakulla et al., 2023). In detail, trace element features fingerprinting a crustal contribution, for example the strongest LREE (Light Rare Earth Element) enrichment and strongest negative Nb anomalies, as exemplified by the lowest Nb/La, are shown by Kalsubai basalts (e.g., La/Yb_N for our samples = 4.4-6.1; Nb/La_N < 0.50; N refers to Primitive Mantle normalized values). These constrast with the slightly less LREE-enriched Bushe sample (Nb/La_N 0.52; La/Yb_N = 3.5) and with the significantly more depleted Wai samples (La/Yb_N = 2.2-2.4; Nb/La_N > 0.8, with the highest values in Ambenali basalts > 1.0).

4.2. Sr-Nd-Pb isotopic compositions

Sr-Nd-Pb isotopic compositions of the studied samples overlap with

Table 1
isotopic compositions of WG basalts. Initial (i) isotopic values are calculated for an age of 66 Ma for all samples. Duplicate Re-Os analyses are reported for samples KAM14-1 and AMB14-2.

sample	MSJ 14-1	MSJ 14-2	MAT 14-2	MAT 14-3	BOR 14-1	BOR 14-2	KAM 14-1	KAM 14-1	AMB 14-2	AMB 14-2	KJA 14-2	AMB 14-6	AMB 14-8	19M-4	AMB 14-10	PAS 14-1
Sub-group	Kalsubai						Lonavala						Wai			
formation	Igatpuri	Igatpuri	Neral	Thakurvadi	Thakurvadi	Thakurvadi	Bushe	Bushe	Poladpur	Poladpur	Poladpur	Ambenali	Ambenali	Mahabaleshwar	Mahabaleshwar	Mahabaleshwar
$^{87}Sr/^{86}Sr$	0.711425	0.712851	0.708520	0.706833	0.717905	0.710042	0.715008		0.706209		0.706990	0.704409	0.704146	0.705069	0.705501	0.705468
$^{87}Sr/^{86}Sr_i$	0.711039	0.712671	0.708099	0.706691	0.717477	0.709779	0.714770		0.706087		0.706748	0.704237	0.703958	0.704908	0.705370	0.705355
$^{143}Nd/^{144}Nd$	0.512235	0.512272	0.512473	0.512246	0.511783	0.511969	0.512184		0.512695		0.512596	0.512879	0.512885	0.512685	0.512459	0.512355
$^{143}Nd/^{144}Nd_i$	0.512168	0.512207	0.512409	0.512184	0.511717	0.511909	0.512111		0.512619		0.512524	0.512802	0.512812	0.512618	0.512396	0.512290
$^{206}Pb/^{204}Pb$	20.074	24.570	19.854	18.015	19.688	17.373	22.534		18.874		18.037	18.368	18.031	17.990	16.929	16.907
$^{207}Pb/^{204}Pb$	15.865	16.350	15.767	15.420	15.760	15.243	16.165		15.659		15.507	15.528	15.459	15.490	15.320	15.281
$^{208}Pb/^{204}Pb$	42.155	45.353	40.600	38.167	40.510	38.192	40.489		39.156		39.042	38.792	38.384	38.329	37.701	38.268
$^{206}Pb/^{204}Pb_i$	19.889	24.094	19.616	17.869	19.526	17.278	22.270		18.704		17.899	18.213	17.826	17.817	16.817	16.794
$^{207}Pb/^{204}Pb_i$	15.857	16.327	15.756	15.413	15.752	15.239	16.152		15.651		15.501	15.521	15.450	15.482	15.314	15.276
$^{208}Pb/^{204}Pb_i$	41.825	44.674	40.248	37.972	40.254	38.032	40.224		38.937		38.812	38.563	38.114	38.095	37.496	38.062
Re ppt		330		255	335	196	325	327	459	483		567	698		230	416
Os ppt		234.3		26.8	33.8	6.5	54.4	43.0	8.4	6.0		14.3	14.5		49.9	129.9
$^{187}Re/^{188}Os$		6.80		46.2	48.3	150.4	28.9	36.8	273.0	415.3		195.8	239.9		22.3	15.5
$^{187}Os/^{188}Os$		0.1484		0.1923	0.2234	0.3763	0.1653	0.1748	0.4461	0.6038		0.3355	0.3844		0.1678	0.1452
2 σ $^{187}Os/^{188}Os$		0.0015		0.0024	0.0023	0.0253	0.0036	0.0030	0.0078	0.1031		0.0158	0.0162		0.0017	0.0025
$^{187}Os/^{188}Os_i$		0.1409		0.1417	0.1703	0.2108	0.1335	0.1343	0.1458	0.1469		0.1202	0.1205		0.1433	0.1282
2 σ $^{187}Os/^{188}Os_i$		0.0017		0.0038	0.0034	0.0104	0.0036	0.0042	0.0125	0.0313		0.0068	0.0073		0.0017	0.0030

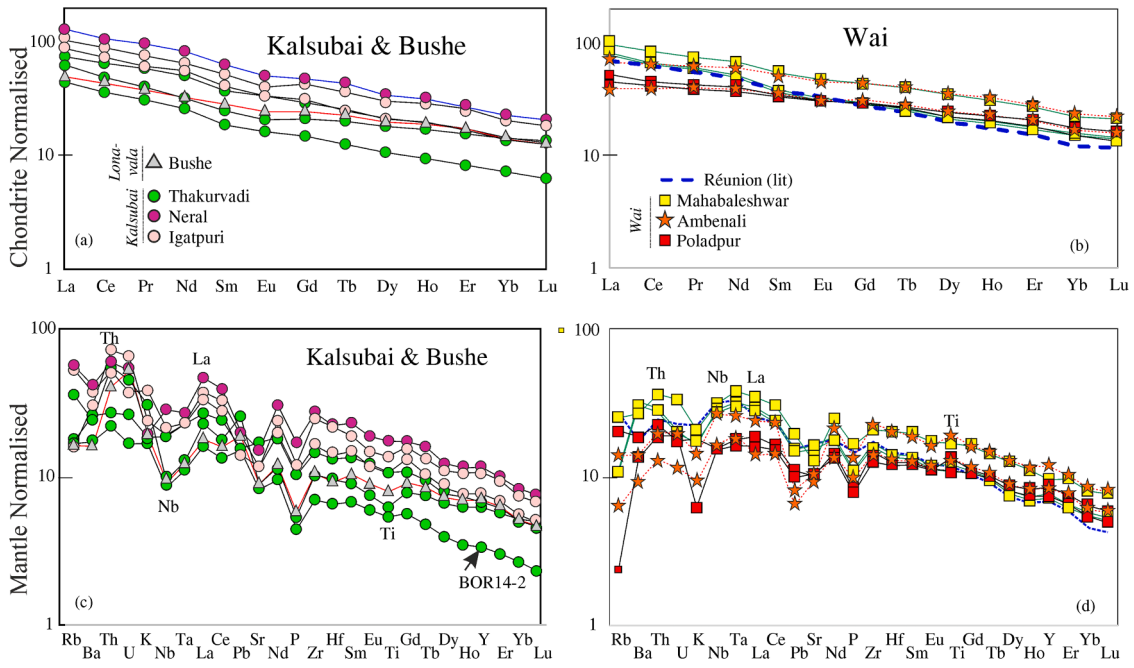

Fig. 2. a, b: Rare Earth Element (REE) concentrations of the studied Deccan basalts normalized to chondritic values (McDonough and Sun, 1995); c, d: Trace elements normalized to Primitive Mantle values (McDonough and Sun, 1995). Réunion data from Halfar et al. (2023).

those of WG basalts from the literature (Fig. 3). The most "depleted" Sr-Nd isotopic compositions, indicating long-term incompatible element depletion of the source, are those of the Ambenali basalts ($^{87}Sr/^{86}Sr_i$ ca. 0.7040 and $^{143}Nd/^{144}Nd_i$ ca. 0.51280, where the suffix i refers to the initial values at 66 Ma; Fig. 3a). They are slightly less depleted than most MORBs and overlap the compositions of present-day Réunion Ocean Island Basalts (OIBs; Schiano et al., 2012; Peters et al., 2016; Halfar et al., 2023; Fig. 3a). Among the other lava flows from the Wai Subgroup, Mahabaleshwar basalts have slightly higher $^{87}Sr/^{86}Sr_i$ coupled with markedly lower $^{143}Nd/^{144}Nd_i$ while Poladpur basalts have higher $^{87}Sr/^{86}Sr_i$ and lower $^{143}Nd/^{144}Nd_i$ than Ambenali samples. Kalsubai and Lonavala samples display a very large range of Sr-Nd isotopic compositions (Fig. 3a), from values similar to the most enriched Wai samples to very high $^{87}Sr/^{86}Sr_i$ (0.71477) and low $^{143}Nd/^{144}Nd_i$ (0.51172). The most radiogenic Sr and least radiogenic Nd isotopic compositions are represented by the Bushe (Lonavala Subgroup) and by some Thakurvadi basalts (Kalsubai), while other Thakurvadi, most Neral (Kalsubai) and Khandala (Lonavala; e.g., Peng et al., 1994) basalts tend to low $^{143}Nd/^{144}Nd_i$ at moderately high $^{87}Sr/^{86}Sr_i$.

Pb isotopic compositions exhibit a very large range (this and previous studies; Fig. 3). The least radiogenic Pb isotopic values (e.g., $^{206}Pb/^{204}Pb_i$ ca. 16.8) are found in Mahabaleshwar, some Neral (e.g., Peng et al., 1994) and some Thakurvadi basalts, while other Thakurvadi, Igatpuri and Bushe basalts reach the most radiogenic Pb isotopic compositions ($^{206}Pb/^{204}Pb_i$ >22). Ambenali basalts have $^{206}Pb/^{204}Pb_i$ (*ca.* 18.3) slightly lower than those of Réunion basalts (*ca.* 18.9; e.g., Halfar et al., 2023).

The isotopic compositions (this and previous studies) show very little or no correlation with major elements (e.g., MgO or SiO_2, Supplementary Information Fig. S4). However, Sr-Nd isotopic compositions are roughly correlated with some incompatible element ratios (e.g., La/Nb, Fig. 4a), while Pb isotopic compositions are weakly correlated with trace element ratios like La/Yb or Th/Nb (Fig. 4b).

4.3. Re-Os isotopic compositions

Re-Os data were obtained on 10 WG samples plus two replicates (Figs. 5, 6; Table 1; all uncertainties are 2σ, cf. Supplementary Information). Literature data shown in Figs. 5, 6 include Re-Os isotopic compositions of 10 Deccan basalts, including one from the WG (probably belonging to the Kalsubai Subgroup) from Allègre et al. (1999), and 38 Deccan samples, including 14 from the WG (7 from Kalsubai, formations not specified, and 7 from Wai: 2 Poladpur, 3 Ambenali, and 2 Mahabaleshwar basalts) from Peters et al. (2017) and Peters and Day (2017). The latter also provided major and trace element data and Sr-Nd isotopic compositions for about half of their samples.

Re and Os contents in our samples vary from ~200 to 700 ppt and from 6 to 235 ppt, respectively (Table 1). Allègre et al. (1999) and Peters et al. (2017) reported similar values for basalts, but picritic samples from Peters et al. (2017) have Os as high as ~900 ppt. Osmium contents are roughly correlated, while Re contents are anti-correlated, with differentiation indices such as Ni content (Fig. 5a and b) reflecting the compatible and incompatible behavior of Os and Re expected during magmatic differentiation. The atypical sample BOR14-2 plots off of these trends.

Measured $^{187}Os/^{188}Os$ values vary from 0.145 to 0.604 (0.119-1.00 for Peters et al., 2017; 0.142-2.06 for Allègre et al., 1999). Measured $^{187}Os/^{188}Os$ and $^{187}Re/^{188}Os$ are positively correlated (Fig. 5c), but as with the data of Peters et al. (2017) a statistically robust isochron could not be defined. This is unsurprising, as the samples were collected from distinct and probably non-cogenetic formations (Fig. 1) with age differences of up to ca. 0.8 Ma. Excellent agreement is observed between the initial ratios ($^{187}Os/^{188}Os_i$ at 66 Ma) of the repeat analyses of each of the two replicated samples, KAM14-1 from the Bushe and AMB14-2 from the Poladpur Formation, despite the fact that in both cases, the measured $^{187}Os/^{188}Os$ and $^{187}Re/^{188}Os$ ratios of the replicates differ substantially (Fig. 5c, d, Table 1). This discrepancy in the measured ratios may be due to the presence of micrometric Platinum Group Element phases that are heterogeneously distributed within the rock. As a result, analyses of different aliquots of the same sample powder may yield different Os concentrations and Re/Os ratios. This is known as the nugget effect. The agreement in the initial ratios not only validates the methodology and but also argues against post-emplacement perturbation of the Re-Os system. Excellent agreement is also found between the $^{187}Os/^{188}Os_i$ (Fig. 5d) of the two analyzed from the Ambenali samples (AMB14-6 and AMB14-8), despite their significantly different and

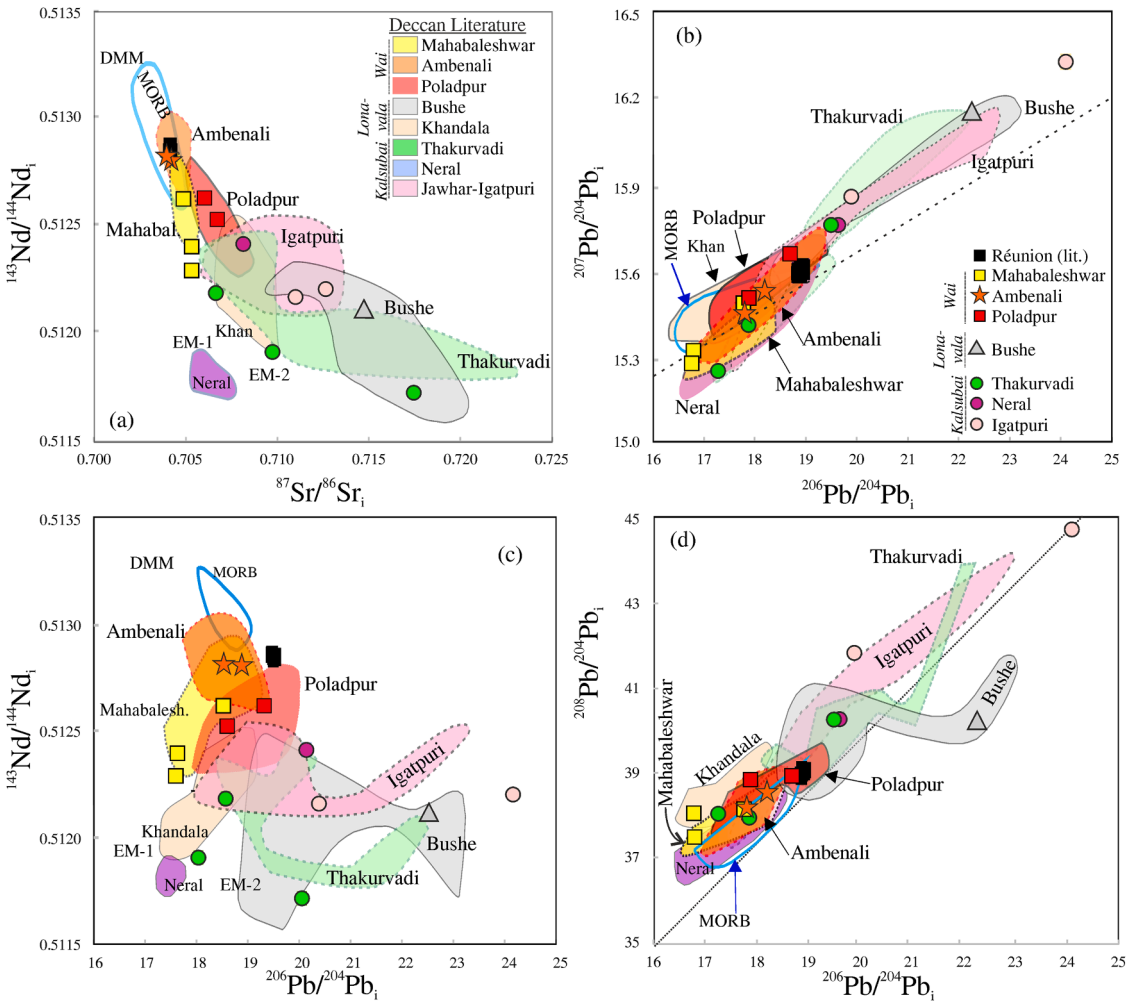

Fig. 3. Sr-Nd-Pb isotopic compositions (all recalculated to 66 Ma) of the studied Deccan basalts (legend in panel b). Fields for each Deccan unit are shown by distinct colors, and include data from Peng et al. (1994), Basu et al. (2020), Marzoli et al. (2022), Hoyer et al. (2023), Pakulla et al. (2023, and references therein). Also shown are present-day isotopic data for Réunion Ocean Island Basalts (e.g. Schiano et al., 2012; Peters et al., 2016; Halfar et al., 2023), and Indian Ocean Normal MORBs (Meyzen et al., 2005 and references therein). Mantle components (Zindler and Hart, 1986) recalculated to 66 Ma: Depleted (DMM) and Enriched 1 (EM-1) and 2 (EM-2). Dashed line in b and d is Northern Hemisphere Reference Line, NHRL (Hart, 1984; not recalculated to 66 Ma). Note that Neral sample (MAT14-2) plots off field of most other Neral samples, but has isotopic compositions similar to those of one Neral basalt analyzed by Basu et al. (2020).

elevated Re concentrations, implying that these distinct Re concentrations date from the time of the emplacement. The higher Re content of AMB14-8 is coupled with a lower Ni content than that of AMB14-6 (Fig. 5b), suggesting slightly different extents of magmatic differentiation.

Initial $^{187}Os/^{188}Os_i$ values of our samples range from 0.120 to 0.211, and vary well beyond limits of uncertainty (Table 1, Fig. 5d). The excellent agreement of the repeat analyses, as well as between the two Ambenali samples, argues that this variation is real, despite the large corrections for radiogenic ingrowth. The lowest $^{187}Os/^{188}Os_i$ values in this study are from the Ambenali basalts (0.120 and 0.121), while the highest are those of two Thakurvadi basalts (0.170 and 0.210, Fig. 5d). The other analyzed basalts (Igatpuri, Thakurvadi, Bushe, Poladpur, Mahabaleshwar formations) range from 0.128 to 0.146. The highest $^{187}Os/^{188}Os_i$ (0.210) is found in the chemically and texturally unusual and possibly slightly altered (LOI 2.84 wt.%) sample BOR14-2. Excluding our samples from the Ambenali and Poladpur flows of the Wai Subgroup, $^{187}Os/^{188}Os_i$ roughly correlates with $1/^{188}Os$ (Fig. 5d). Our Poladpur and Ambenali samples plot below this trend, with the latter having less radiogenic compositions than both the estimated primitive upper mantle (PUM; present-day $^{187}Os/^{188}Os = 0.1296 \pm 0.0008$; Meisel et al., 2001, Fig. 6) and Réunion OIBs ($^{187}Os/^{188}Os =$ 0.131-0.137; Schiano et al., 2012, Fig. 6).

Initial Os vs. Sr-Nd-Pb isotopic composition plots show weak correlations (Fig. 6), but, in general, high $^{187}Os/^{188}Os_i$ (> 0.15) are found in samples having radiogenic Sr and unradiogenic Nd (e.g., the Thakurvadi samples: BOR14-1 and BOR14-2). On the contrary, some samples with very enriched Sr-Nd-Pb isotopic compositions have only moderately high $^{187}Os/^{188}Os_i$ (e.g., the Igatpuri and Bushe samples: 0.141 and 0.134).

5. Discussion

In line with numerous previous works on the Deccan (e.g., Mahoney et al., 1982, 2000; Cox and Hawkesworth, 1985; Peng et al., 1994; Peters et al., 2017; Basu et al., 2020; Pakulla et al., 2023; Hoyer et al., 2023), this study highlights significant differences in geochemical compositions among the Kalsubai, Lonavala, and Wai Sub-group basalts, as well as among individual formations of each subgroup. In the following paragraphs we use the geochemical data, especially the new Re-Os isotopic compositions, to constrain the possible contributions of crustal, SCLM, and sub-lithospheric mantle components to the petrogenesis of the WG magmas.

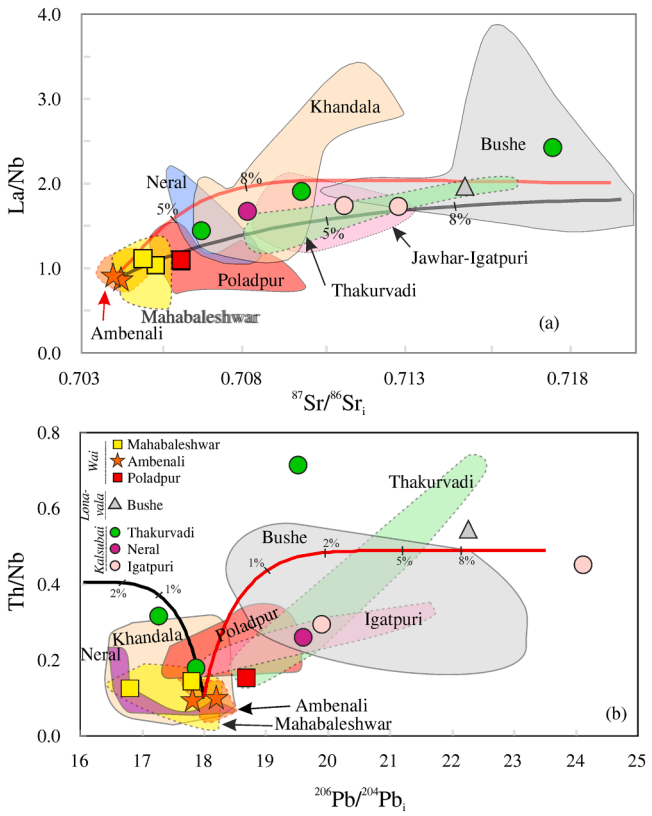

Fig. 4. Trace element ratios (La/Nb and Th/Nb, respectively) vs initial Sr and Pb isotopic compositions of the studied basalts. Curves show the calculated evolution paths of a parental Ambenali magma, which assimilates one of two distinct felsic upper crustal rocks with either radiogenic (red) or unradiogenic (black) Pb isotopic composition (compositions and parameters used in the assimilation modelling are listed in Supplementary Information Table S3, further details on the calculations are reported in the main text). Tick marks show wt.% of assimilated crust. Literature data for the WG are from Basu et al. (2020) and Pakulla et al. (2023, and references therein).

5.1. Crustal contamination

The crust under the WG is mainly formed by rocks from the Dharwar craton (see Supplementary Information). The available isotopic data for Archean to Proterozoic felsic and mafic rocks from this craton show a very large range of compositions ($^{87}Sr/^{86}Sr_i$ from 0.7023 to > 1.0, $^{143}Nd/^{144}Nd_i$ 0.5120-0.5103; $^{206}Pb/^{204}Pb_i$ 14.5-23.3, values recalculated to 66 Ma; references in the Supplementary Information, ranges shown in Fig. S5). Re-Os isotopic data are not available for the Indian basement, but possible compositions can be hypothesized, considering felsic and mafic rocks of Archean to Paleoproterozoic age. Typically, the Os content of the felsic upper crust is ca. 5-50 ppt, with average $^{187}Re/^{188}Os = 34.5$ (Peucker-Ehrenbrink and Jahn, 2001; Rudnick and Gao, 2014) and therefore $^{187}Os/^{188}Os \geq 1.0$ is expected for Mid Proterozoic to Archean rocks. The Os content and $^{187}Os/^{188}Os$ for the mafic lower continental crust were estimated to be 30 ppt and 0.8, respectively (*cf.* Saal et al., 1998).

The modelling of major element variations during open-system magma differentiation was carried out using the Magma Chamber Simulator code (MCS; Bohrson et al., 2020) and the results are presented in the Supplementary Information Fig. S3. Considering that high-Mg rocks with compositions representative of melts are rare in the WG and absent in the Wai Subgroup, the starting compositions considered (Supplementary Information Table S2) are a high-Ti Thakurvadi basalt, Kalsubai Subgroup (JEB15; Basu et al., 2020), and a high- and a low-Ti picrite from the Northern Deccan (Melluso et al., 2006). The crustal assimilants are a granulite and a granitoid with 54 and 69 wt.% SiO_2 to represent the lower and upper crust, respectively. Calculated liquid lines of descent overlap only a limited number of WG basalt compositions (present study and literature data) confirming that several distinct parental magmas would be required to reproduce the range of WG basalt compositions. In particular, the lack of near-primitive Wai magmatic rocks hinders the modelling of basalts from this Subgroup. In the MCS modelling, crustal assimilation occurs only after crystallization of the parental magma has provided sufficient energy to heat the crust above its solidus temeperature. Therefore, if the assimilated crust initially was ca. 200°C below its solidus crustal assimilation would only occur in fairly evolved magmas (MgO <5 wt.%) with a maximum of ca. 3 wt% assimilation in basaltic andesites. On the contrary, an initially hotter (near-solidus) crust could have been assimilated by slightly less evolved magmas (MgO ca. 7 wt.%) reaching a maximum of ca. 9 wt.% assimilation in basaltic-andesite magmas.

Isotopic ratios and trace element variations were modelled using the EC-AFC, energy-constrained assimilation and fractional crystallization code of Spera and Bohrson (2001), which models the fractional crystallization process and concurrent assimilation of crustal melts, with the parameters listed in Supplementary Information Table S3. The choice of using EC-AFC to model trace element and isotopic variations is discussed in the Supplementary Information. The models shown in Figs. 4 and 7 start from an Ambenali basalt and from a low-Ti picrite (Melluso et al., 2006; Supplementary Information Tables S3). In the Supplementary Information Figs. S7, S8 we show EC-AFC modelling results starting from parental magmas having the composition of a Réunion basalt and of a high-Ti picrite from the Northern Deccan (data from Peters et al., 2017). The Ambenali basalt and the Northern Deccan high-Ti picrite have unusually unradiogenic $^{187}Os/^{188}Os$ ratios for mantle-derived melts (0.120 and 0.119 respectively), which will maximize the calculated amount of crustal assimilation when these parental compositions are assumed. In the EC-AFC model, crustal melting and consequent assimilation starts once the crustal rocks reach their solidus, e.g., after ca. 40% crystallization of the parental magma if the assimilated crust initially was ca. 200°C below its solidus. We considered several possible assimilants (Figs. 5, 7; Supplementary Information Table S3, Fig. S6), consistent with published Sr-Nd-Pb data and estimated Os compositions for crustal rocks from central-southern India (cf. Supplementary Information).

The crustal assimilation EC-AFC modelling (Figs. 4, 5, 7) does not aim to reproduce the compositions of every Deccan lava flow or formation and several uncertainties need to be considered: a) the crustal and parental magma compositions as well as thermal and compositional parameters used in the modelling are necessarily only an approximation of the true values (see the Supplementary Information for a discussion on the selection of input parameters and on modelling done with other thermal and chemical parameters for the parental basalt and crust). In particular, it is well known that the WG lavas from the 11 formations cannot be considered as cogenetic, but require several distinct parental magma compositions (see the above discussed major element modelling); b) we mainly focus on the relatively few samples analyzed for $^{187}Os/^{188}Os_i$, which may differ slightly in composition from other basalts from the same formation; c) the assimilation process might have included processes not modelled here, i.e., xenolith digestion (Tegner et al., 2005), or selective contamination by low degree partial melts of low-solidus crustal minerals (e.g., Haase et al., 2019). Nonetheless, the assimilation trends calculated with the EC-AFC modelling reasonably well constrains the general range of open-system evolution of Deccan magmas.

Assimilation of Archean to Proterozoic mafic (amphibolitic or granulitic) crustal rocks would significantly affect the Os isotopic compositions even at low degrees of assimilation, since these lithologies are relatively Os-rich (*cf.* the blue curves in Figs. 5d and 7a, c, e). For example, *ca.* 1.7 wt.% assimilation of amphibolite or mafic granulite ($^{187}Os/^{188}Os_i = 0.8$; [Os] = 30 ppt; $^{87}Sr/^{86}Sr = 0.710$; $^{143}Nd/^{144}Nd =$

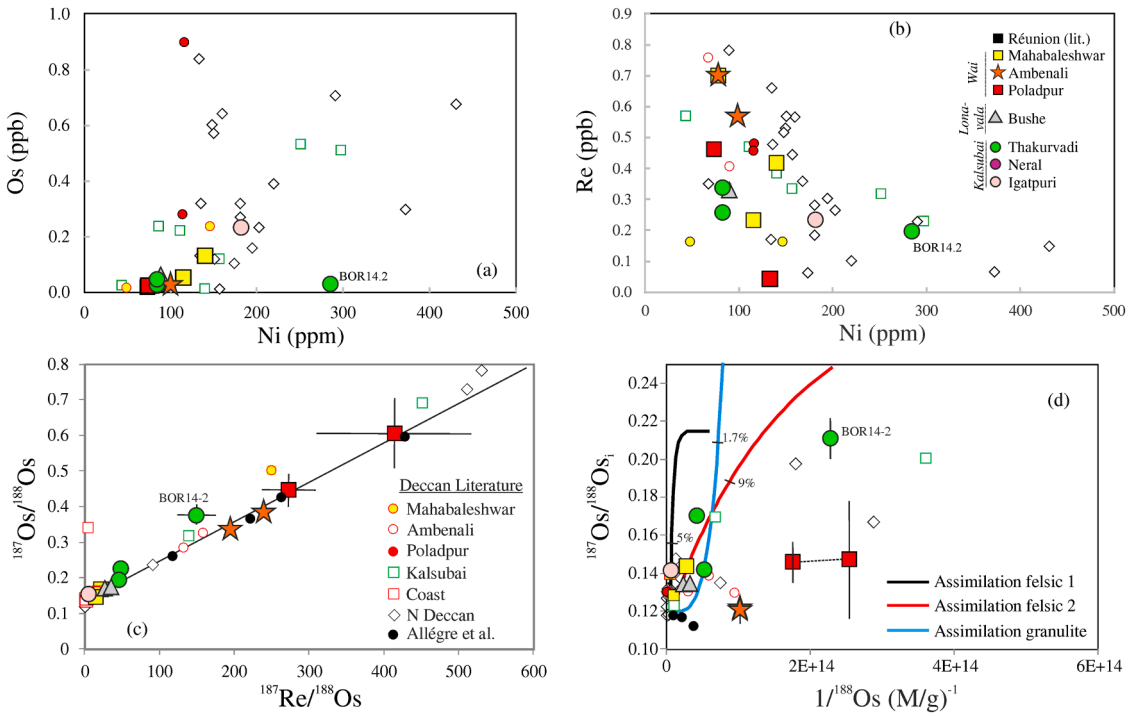

Fig. 5. Re-Os data for Deccan basalts (present study; literature data from Peters et al., 2017; Peters and Day, 2017; data from Allègre et al. (1999), only in c, d). (a, b): Os and Re (ppb) vs. Ni (ppm) content. c) $^{187}Os/^{188}Os$ (measured values) as function of $^{187}Re/^{188}Os$. A 66 Ma reference line is shown, assuming an initial $^{187}Os/^{188}Os$ ratio of 0.133 (typical composition of Réunion basalts; Schiano et al., 2012). d) Initial Os isotopic ratios ($^{187}Os/^{188}Os_i$) as function of Os content, shown as $1/^{188}Os$ (M/g)$^{-1}$. Excellent agreement in $^{187}Os/^{188}Os_i$ is observed between repeat analyses, indicated by dashed lines, for the two samples tested (Bushe sample KAM14-1 and Poladpur sample AMB14-2), despite differences in Os concentration likely due to the *nugget effect*. Blue, red, and black curves are calculated compositions of parental Ambenali-like magma contaminated by granulitic and two distinct granitic crustal rocks, respectively (see Supplementary Information for details on assimilation modelling and parameters). In panel d, tick marks show wt.% of assimilated crust. In all panels, analytical uncertainties are either shown by thin black lines or are smaller than the size of the symbol. Initial Os isotopic ratios for samples from Allègre et al. (1999) recalculated using ^{187}Re decay constant value of 1.666×10^{-11} yr^{-1} and assuming an age of 66 Ma, yielding $^{187}Os/^{188}Os_i$ ranging from 0.089 (an impossible value) to 0.142.

0.5119; $^{206}Pb/^{204}Pb = 18$; see the Supplementary Information Fig. S6f for modelling done with different $^{187}Os/^{188}Os$ of mafic crustal compositions) would increase $^{187}Os/^{188}Os_i$ from 0.120 to ca. 0.22, i.e., cover the entire range of the WG basalts from this study and from Peters et al. (2017; considering only samples with LOI < 3.0 wt.%). For the same degree of assimilation, the change of Sr and Nd isotopic composition of the contaminated magma would be almost negligible ($^{87}Sr/^{86}Sr$ from 0.7040 to 0.7043 and $^{143}Nd/^{144}Nd$ from 0.5128 to 0.5127) and would not reproduce the enriched compositions of the Kalsubai and Lonavala samples (Fig. 7). Therefore, the entire range of isotopic compositions of WG basalts cannot be readily explained by the assimilation of mafic rocks alone.

We tested two potential felsic contaminants within the spectrum displayed by the compositions of the Dharwar crustal rocks with, respectively, unradiogenic and radiogenic $^{206}Pb/^{204}Pb_i$ (15 and 25) and moderately to highly radiogenic $^{87}Sr/^{86}Sr_i$ (0.730 and 0.770; $^{143}Nd/^{144}Nd = 0.510$ and 0.511, repsectively; Supplementary Information). The four calculated assimilation curves (Fig. 7) starting from the two parental magmas bracket most of the observed isotopic compositions of Deccan basalts from this and previous studies. Starting from the Ambenali composition, assimilation of felsic rocks with unradiogenic Pb and moderately radiogenic Sr isotopic compositions (AFC-1 curve in Fig. 7) would produce basalts with isotopic compositions similar to those of the Mahabaleshwar Formation for *ca.* 1 to 3 wt.% assimilation. Starting from the low-Ti picrite, assimilation of felsic contaminants with very radiogenic Pb and Sr isotopic compositions (low-Ti AFC-2 curve in Fig. 7) would reasonably well reproduce the isotopic compositions of the Bushe basalt and of the most enriched Kalsubai basalts for less than 5 wt.% and up to *ca.* 7-9 wt.% assimilation, respectively. Similar results in terms of amounts of assimilation were obtained when considering the Réunion or Northern Deccan high-Ti picrite as parental magmas (Supplementary Information Fig. S8). The EC-AFC modelling assumes bulk assimilation of the contaminant, and it could be argued that selective assimilation favoring more fusible phases is more realistic. Sulfides, the main hosts of Os in silicate rocks, have low melting temperatures and typically occur as intergranular trace phases, and thus are likely to be easily mobilized during crustal melting. Thus crustal Os may be disproportionately represented in the assimilated melt, implying the amounts of crustal assimilation may have been even lower than those we calculated.

The large scatter of Sr-Nd-Pb isotopes and major and trace element ratios for the WG basalts (Figs. 3, 5–7) suggests that the crustal contamination process involved distinct parental magmas (likely more than those considered here) possibly issued from distinct mantle sources (Melluso et al., 2006). Moreover, several distinct felsic crustal rocks of different age and composition (e.g., the assimilants considered in the AFC1 and AFC2 curves in Figs. 4, 7) may have been assimilated in distinct portions of the Dharwar craton. Vanderkluysen et al. (2011) have shown that the feeder dykes of the WG lavas probably migrated over time, as most Igatpuri, Thakurvadi and Bushe flows are chemically similar to dykes from the Narmada-Tapi rift, whereas most Wai subgroup flows are correlated with dykes from the Central Deccan dyke swarm and from the coast south of Mumbai (Fig. 1a).

In agreement with previous studies (e.g., Mahoney et al., 1982; Peng et al., 1994; Capriolo et al., 2024; Chatterjee, 2024), our results suggest that several WG basaltic magmas, particularly those of the Kalsubai and Lonavala subgroups are contaminated by mostly felsic continental crust. However, unlike what would be expected, given the very radiogenic Sr and unradiogenic Nd isotopic compositions of, e.g., the Igatpuri, Thakurvadi or Bushe basalts, the available $^{187}Os/^{188}Os_i$ data suggest that

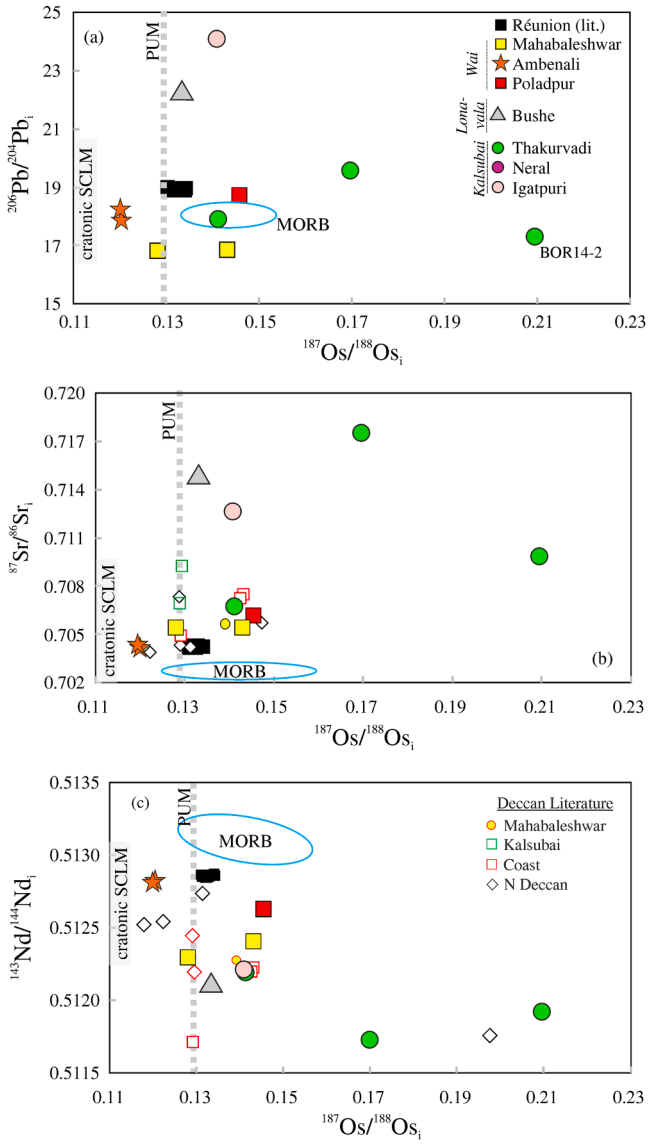

Fig. 6. Initial Sr-Nd-Pb vs. Os isotopic compositions of Deccan basalts (this study, Peters et al., 2017, and Peters and Day, 2017) compared with Réunion OIBs (Schiano et al., 2012) and Indian MORBs (field with blue contour; Gannoun et al., 2016). As the latter may be modified by incorporation of altered oceanic crust, the Os isotopic composition of the shallow asthenospheric mantle may be better represented by whole-rock abyssal peridotites or Os-rich sulfides in MORBs ($^{187}Os/^{188}Os$ = 0.127 ±0.015 and 0.129 ± 0.005, respectively; Gannoun et al., 2016) or, alternatively, by the estimated Primitive Upper Mantle value (PUM, present-day value = 0.1296 ± 0.0008; Meisel et al., 2001; thick dashed gray line). The gray field shows the typical Os isotopic composition of the Archean Sub-continental lithospheric mantle (SCLM: $^{187}Os/^{188}Os$ ca. 0.105 to 0.115; Carlson, 2005).

crustal contamination rarely exceeded 8 wt.% and was generally low (<3 wt.%) for most WG basalts investigated here. Such degrees of crustal contamination are significantly lower than those calculated in previous geochemical studies (10-25 wt.% assimilation) of Deccan basalt (e.g., Peng et al., 1994; Mahoney et al., 2000; Melluso et al., 2006). A significant proportion of WG basalts, including those from the Wai Subgroup, in particular the Ambenali Formation, but also Deccan basalts and picrites from the northern sub-provinces (Allégre et al., 1999; Peters et al., 2017) have $^{187}Os/^{188}Os_i$ < 0.130 and are thus virtually uncontaminated by the continental crust. This is consistent with major element modelling (Supplementary Information), which indicates that assimilation of > 8 wt.% of Dharwar crustal rocks would produce contaminated magmas with significantly higher SiO_2 and lower MgO than most WG basalts. However, due to the extremely enriched Sr-Nd-Pb isotopic compositions of the Dharwar rocks, even very low degrees of crustal contamination could significantly modify the isotopic composition of the WG basalts. Therefore, the involvement of enriched mantle components, related to low-degree melts from the SCLM or to recycled crustal components in the sub-lithospheric mantle proposed by some authors (e.g., Peters et al., 2017; Basu et al., 2020) is difficult to detect, at least for the evolved WG basalts studied here. For this reason, in the following sections, we model the mantle source of only those magmas that appear to be uncontaminated, as suggested by their low $^{187}Os/^{188}Os_i$ (< 0.130).

5.2. Sub-lithospheric and lithospheric mantle components in Wai basalts

In this section, we model the potential contribution of the SCLM for Deccan basalts (Ambenali and some Northern Deccan samples from Peters et al., 2017) that have significantly lower $^{187}Os/^{188}Os$ values than those of Indian Ocean MORBs and Réunion OIBs (Fig. 6). The Sr-Nd-Pb isotope composition of the SCLM is provided by low degree melts from the lithospheric roots of the Dharwar craton (e.g., Simonetti et al., 1998; Melluso et al., 2002). Given its Archean age and generally refractory character, the SCLM underlying the Dharwar craton is expected to have very low $^{187}Os/^{188}Os$ in the range of 0.105-0.115, consistent with typical compositions of the Archean SCLM world-wide (Carlson, 2005) and with analyses of Archean chromitites from a layered intrusion in the western Dharwar craton ($^{187}Os/^{188}Os$ 0.105-0.107; Santosh et al., 2020). The SCLM underlying Proterozoic suture zones between Archean blocks would be expected to have only moderately higher $^{187}Os/^{188}Os$, mostly 0.110-0.124 (e.g., Janney et al., 2010). These unradiogenic Os compositions are coupled with very high Os contents, typically ~ 2-4 ppb for cratonic peridotites (Aulbach et al., 2016). Paradoxically, the low $^{187}Os/^{188}Os$ of the cratonic SCLM, indicative of ancient depletion, are nearly always associated with strongly enriched Sr-Nd-Pb isotope ratios, reflecting long-term metasomatic enrichment in highly incompatible elements. More than 90% of global xenoliths from Archean SCLM have $^{143}Nd/^{144}Nd$ ratios <0.5128 (Reisberg and Aulbach, 2025) similar to those of alkaline-carbonatitic rocks from India interpreted as low-degree melts from the SCLM (e.g., Simonetti et al., 1998; Melluso et al., 2002).

Potential sublithospheric mantle components involved in the genesis of the Deccan basalts include the Réunion mantle plume and the shallow convecting asthenospheric mantle. For Sr, Nd and Pb, present-day N-MORBs are considered as representative of the shallow asthenospheric component. The Os isotopic compositions of most MORBs have been altered by interaction with seawater, so the average $^{187}Os/^{188}Os$ of abyssal peridotites or of Os-rich sulfides exsolved from MORB (0.127 ± 0.015 and 0.129 ± 0.005, respectively; Gannoun et al., 2016) are likely to be more representative of the mean asthenospheric value, and are close to the estimated PUM value (0.1296 ± 0.008; Meisel et al., 2001). The composition of the mantle-plume component may be similar to that of present-day Réunion-Mascarene Archipelago OIBs (e.g., $^{187}Os/^{188}Os$ 0.131-0.134; Schiano et al., 2012; Peters et al., 2016).

As shown in previous studies, Sr-Nd-Pb isotopic compositions and trace element ratios similar to those of Ambenali basalts can be obtained by mixing of melts from the shallow convecting-mantle (ca. 40-60%) and from the Réunion mantle plume (e.g., Melluso et al., 2006). However, the low $^{187}Os/^{188}Os_i$ of Ambenali basalts cannot be achieved by a simple MORB-Réunion mixing and requires an additional low-$^{187}Os/^{188}Os$ component. Such a component exists in the SCLM. However, assimilation of SCLM peridotite bulk rocks is quite unlikely considering the refractory nature of these mantle rocks. A more physically plausible scenario may be assimilation of low degree (strongly alkaline) melts from the SCLM, which are expected to have low $^{187}Os/^{188}Os$ coupled with enriched Sr-Nd isotopic ratios and high Sr-Nd trace element contents (e.g., Simonetti et al., 1998; Melluso et al., 2002). However, such

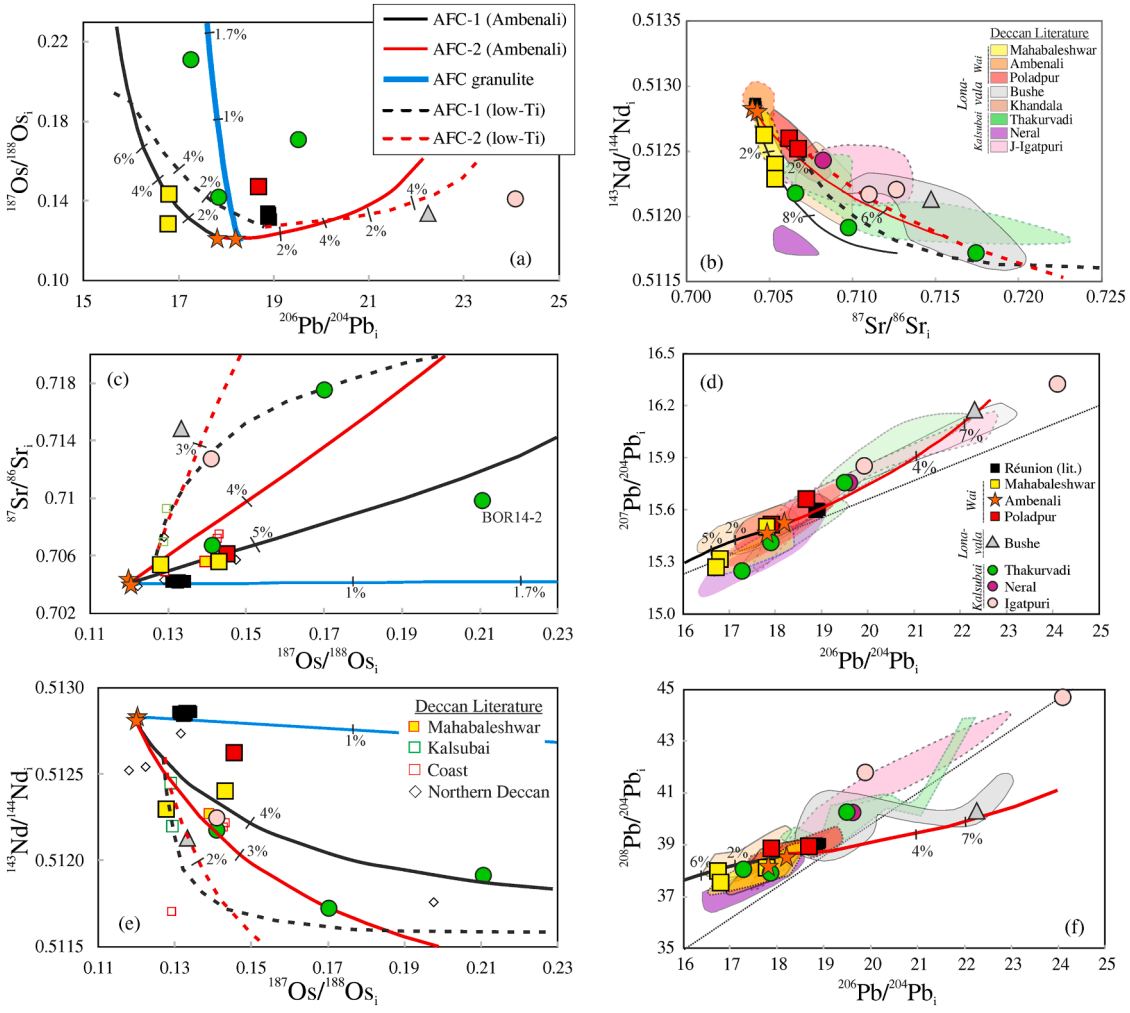

Fig. 7. Isotopic compositions (recalculated to 66 Ma) with calculated EC-AFC trends starting from a parental basalt with isotopic compositions equal to our Ambenali basalts (thick lines) or a low-Ti picrite (dashed lines; Melluso et al., 2006) contaminated by one of two distinct felsic components (red and black lines) or one mafic contaminant, granulite (blue line, shown only in a, c, e, as the effects of granulite assimilation appear almost negligible for the Sr-Nd-Pb systematics). Modelling details reported in text, parameters are in Supplementary Information Table S3. Tick marks show wt.% of assimilated crust. See Supplementary Information for a discussion on the isotopic composition of BOR14-2, the sample with highest $^{187}Os/^{188}Os_i$. Literature data for Os isotopic compositions for Deccan and Réunion are as in Fig. 5, while Sr-Nd-Pb isotopic fields for Deccan WG formations are as in Fig. 3.

melts are also expected to have the low Os contents typical of intraplate alkaline magmas (Gannoun et al., 2016). Therefore, such SCLM melts would rapidly enrich the Sr-Nd isotopic composition of the sublithospheric magmas, but would not significantly change their $^{187}Os/^{188}Os_i$.

Alternatively, the low $^{187}Os/^{188}Os$ SCLM signature may not be derived from bulk peridotites or low degree melts, but primarily from sulfides. Sulfides in the SCLM are low solidus phases potentially very rich in Os (Harvey et al., 2011) and somewhat enriched in Pb (Hart and Gaetani, 2006; Harvey et al., 2016). Therefore, selective contamination of the Réunion-DMM mixture magmas by sulfides in the lithosphere would have a negligible effect on the Sr-Nd isotopic composition of contaminated asthenospheric magmas, but could drive the $^{187}Os/^{188}Os$ towards significantly less radiogenic values. This process might also explain the moderate but systematic difference between the Pb isotopic composition of Ambenali and Réunion magmas, although further investigation would be required to support this suggestion.

6. Why do the Deccan Traps and other LIP basalts typically show low degrees of crustal contamination?

The evolved composition of most LIP basalts (MgO < 10 wt.%), including those from the WG, requires about 30-60 wt.% crystal fractionation from parental primary mantle-derived magmas (Cox and Hawkesworth, 1985; Marzoli et al., 2022; Chatterjee, 2024; MCS modelling in the Supplementary Information). This implies that the crustal roots of LIPs include large amounts of gabbroic rocks, in particular in the lower crust near the Moho (e.g., Mittal et al., 2021). Fluxing of CO_2 from mantle-derived basalts, combined with the latent heat of crystallization released by the fractionating magma, and the high temperatures of plume-related LIP basalts likely promote crustal melting and assimilation (Cashman et al., 2017; Capriolo et al., 2024). Our new data, combined with those from several previous studies on the Deccan, show that some crustal contamination affected most WG basalts. However, the Re-Os data indicate that the degrees of crustal assimilation usually remained low. Picritic and basaltic magmas from several other Mesozoic and Cenozoic LIPs also show evidence for generally unradiogenic Os isotopic compositions and thus low contributions of assimilated crustal rocks (Cuciniello et al., 2010; Rocha Junior et al., 2012; Heinonen et al., 2014; Callegaro et al., 2017; Day et al., 2024; Fig. 8). This seems to be independent regardless of the age, composition, and thus fertility of the crust on which these continental LIPs were emplaced. Here, we propose a new conceptual model to explain such low levels of contamination in LIP basalts associated with high magma production rates.

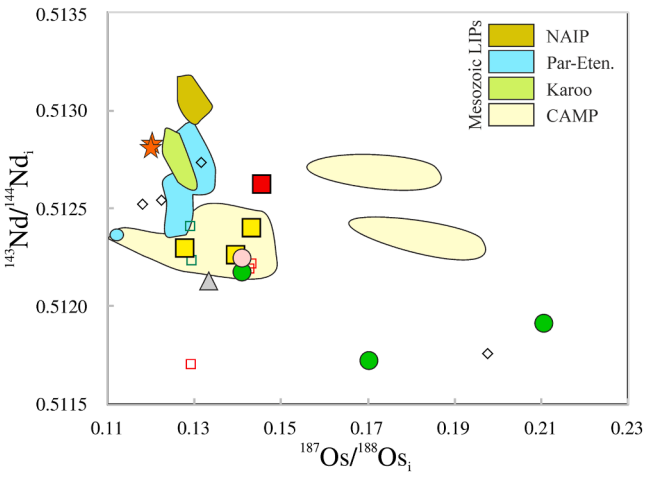

Fig. 8. Nd vs Os isotopic compositions for Mesozoic LIPs (coloured fields) and Deccan basalts (for the Deccan, same symbols as in previous figures). Data for Mesozoic LIPs: NAIP, North Atlantic Igneous Province (*ca.* 60 Ma): Day et al. (2024); Paramà-Etendeka (*ca.* 132-135 Ma): Day et al. (2024), Rocha Junior et al. (2012); Karoo, Dronning Maud Land (*ca.* 180 Ma): Heinonen et al. (2014; and references therein); CAMP, Central Atlantic Magmatic Province (*ca.* 201 Ma): Callegaro et al. (2017; and references therein). All $^{187}Os/^{188}Os$ are initial values for each LIP.

EC-AFC modelling for major elements and for trace element and isotope ratios suggests that the degree of assimilation in WG basaltic magmas remains low (< 3 wt.% of starting magma mass) except when the initial temperature of the crustal assimilant is close to its solidus temperature (in which case assimilation may reach a maximum of 8-9 wt.% in evolved magmas, i.e., basaltic andesites). Heating of the crust by intruding magma is generally a relatively slow process because conductive heat transfer is sluggish in silicate rocks. Numerical models (Annen et al., 2006; Karakas and Dufek, 2015) highlight the importance of magma intrusion rates on crustal melting and indicate that a relatively long incubation time is expected before the solidus temperature of the crust is reached. These models predict an incubation time of *ca.* 0.2 and 0.6 Ma in the lower and upper crust, respectively, in arc settings with typical arc intrusion rates (5 mm/year, i.e., 5 km thick basaltic sill intruded in 1 Ma; Annen et al., 2006) and > 0.8 Ma in continental rift settings (Kararkas and Dufek, 2015).

As indicated by paleomagnetic studies and by Hg analyses of coeval sediments, LIP lavas, including those from the Deccan, were emplaced as a series of very productive short-lived eruptions, each possibly lasting less than a century (e.g., Hoyer et al., 2023; Fendley et al., 2019; Kent et al., 2024) and involving some 50-250 km^3 basaltic magma per year (Self et al., 2022). During such short time intervals, only a very small volume of crustal wall-rocks can be heated up to their solidus by conductive heating, even if the amount of intruded LIP magma was very high. Following Annen et al. (2006), felsic shallow crustal rocks would start melting after ca. 100-500 years only if the intrusion rate of LIP-related mantle-derived magma is *ca.* 80-100 mm/year. Therefore, during LIP emplacement crustal contamination may be effective only when the magma production rate is very high, continuous and prolonged over several centuries, whereas voluminous but brief magma pulses (*ca.* 100 years; e.g., Fendley et al., 2019; Kent et al., 2024) would not favor significant crustal contamination. Moreover, according to Mittal et al. (2021) the magmatic plumbing system of the Deccan Traps and probably of most LIPs was not formed by large magma chambers, but by a series of rather small and separated transcrustal magma mush reservoirs (Marzoli et al., 2022), which fed distinct fissure vents erupting at about the same time. In such a scenario, the rate of magma intruded per unit area would probably not be much larger than that observed in arc- or rift-related volcanoes.

Finally, LIP magmatism is frequently interpreted as resulting from the impingment of a mantle-plume under a continental plate thus producing a time-related migration of the magmatic plumbing systems and vents. In the case of the Deccan, such migration is supported by decreasing ages from the Northern (Tholt et al., 2023) to the Main Deccan (e.g., Schoene et al., 2019; Sprain et al., 2019). As shown by Vanderkluysen et al. (2011), the feeder dyke systems migrated from the end-Cretaceous emplacement of the Kalsubai and Lonavala to the early Paleogene eruption of Wai basalts. We therefore speculate that, in the case of the Deccan, the thermal anomaly associated with the impinging mantle plume did not persist over the same basement area, but rapidly shifted southward, preventing significant localized heating of the Dharwar continental crust and thus limiting crustal assimilation.

The complexity of the assimilation process is furthermore highlighted by significant major and trace element and Sr-Nd-Pb-Os isotopic differences among basalts from individual formations, e.g., Jawhar-Igatpuri, Neral, Thakurvadi, Bushe or Mahabaleshwar formations (our data; Peters et al., 2017; Hoyer et al., 2023; Figs. 3, 4, 7). This suggests involvement for single formations of distinct crustal contaminants, but also distinct degrees of contamination and possibly distinct parental magmas. This would be consistent with synchronous eruptions from distinct vents that tap distinct magma plumbing systems traversing different crustal sections.

Interestingly, a progressive increase of the degree of crustal contamination was observed for the earliest erupted Columbia River LIP basalts, the Miocene Steens basalts (Moore et al., 2020). During emplacement of the Lower Steens basalts, frequent magma injections of overall short duration suppressed crustal contamination by refilling the chamber with uncontaminated melt. On the contrary, the Upper Steens basalts erupted at lower rates and assimilated larger amounts of the shallow crust, which had been previously heated by the Lower Steens magmas (Moore et al., 2020). Detailed studies on the WG will be required to test if a similar scenario could explain the isotopic variability within individual WG formations, some of which are comparable in terms of duration, areal extent, and magma volume to the entire sequence of the Steens basalts (Kasbohm and Schoene, 2018; Moore et al., 2020).

Our proposed interpretation of the apparently low degrees of crustal assimilation for LIP basaltic magmas does not explain why Kalsubai and Lonavala magmas tend to be more contaminated than Wai magmas. At first glance, this might be explained by the fact that the Kalsubai and Lonavala magmas were erupted first, and thus depleted the crust in the most fusible and enriched components, prior to the passage of the Wai magmas. However, unlike in the WG, in the northern Deccan (e.g., the Malwa Plateau) the least contaminated magmas erupted before the most contaminated ones (Haase et al., 2019; Tholt et al., 2023). This suggests that the degree of crustal assimilation in the Deccan is not simply due to time-related changes of crustal fertility and progressive removal of the fusible components of crustal contaminants. We suggest that the different degrees of contamination of Kalsubai and Lonavala vs. Wai formations may be viably explained by the distinct emplacement tempos of the different Subgroups and by the distinct durations of quiescent phases between successive eruptions. Wai eruption pulses were quite voluminous, consistent with the large total volume of these formations and with the geometry and size of their sheet lobes (Self et al., 2022). However, these eruptions were interrupted by relatively prolonged and frequent volcanic hiatuses as indicated by the numerous non-volcanic layers (the so-called red boles, many of them most likely being palaeosols or sedimentary interlayers; e.g., Widdowson et al., 1997) interstratified among Wai lava flows (Fig. 1b). By contrast, for the earlier formations, eruptions were not interrupted by as many hiatus events, favoring a more continuous heating of the crust, thus increasing the efficacy of the crustal assimilation process.

7 Conclusions

Combined major and trace element and Sr-Nd-Pb-Os isotopic data provide important constraints on the genesis of Deccan flood basalts from the Western Ghats. Sr-Nd isotopic compositions similar to present-day Réunion mantle plume basalts are evident only in Ambenali basalts, which however have Pb and Os isotopic compositions slightly less radiogenic than Réunion basalts. The low $^{187}Os/^{188}Os_i$ of Ambenali basalts is tentatively interpreted as reflecting limited interaction with peridotites of the sub-continental lithospheric mantle, or more specifically by SCLM sulfides. Some crustal contamination is apparent in the Sr-Nd-Pb isotope compositions of most other WG formations, especially for basaltic rocks from the Kalsubai and Lonavala Subgroups. However, most of these lavas have relatively low $^{187}Os/^{188}Os_i$ indicating a dominant mantle signature and suggesting that Deccan basalts have experienced little to very little crustal contamination. Similar Os isotopic compositions suggest that basalts from other LIP have also suffered minor to negligible degrees of crustal contamination. Thus despite the very high magma production rates and volumes of erupted magmas observed in LIPs, the very short duration of single volcanic pulses interspersed with relatively long volcanic hiatus periods may have hindered significant melting of basement rocks and thus contamination of these basaltic magmas.

CRediT authorship contribution statement

A. Marzoli: Writing – original draft, Investigation, Conceptualization. **L. Reisberg:** Writing – review & editing, Funding acquisition, Formal analysis, Data curation, Conceptualization. **M. Capriolo:** Writing – review & editing, Formal analysis. **S. Callegaro:** Writing – review & editing, Funding acquisition. **P.R. Renne:** Writing – review & editing, Investigation, Funding acquisition. **M. Chiaradia:** Writing – review & editing, Methodology, Formal analysis. **C.M. Meyzen:** Writing – review & editing. **S. Self:** Writing – review & editing, Investigation. **L. Vanderkluysen:** Writing – review & editing, Investigation. **A. Boscaini:** Writing – review & editing, Software, Methodology.

Declaration of competing interest

The authors declare that they have no known competing financial interests or personal relationships that could have appeared to influence the work reported in this paper.

Acknowledgments

PRR acknowledges support from the US National Science Foundation (NSF grants EAR-1736737 and EAR-1615021), the Esper S. Larsen Jr. fund of UC Berkeley, and the Ann and Gordon Getty Foundation. SS acknowledges support from US NSF and the Esper S. Larsen Jr. fund of UC Berkeley. SC acknowledges funding from the Norwegian Research council (grant 301096). LV acknowledges support from NSF grant IES-1615003. Marie Laure Rouget (Brest) and Daria Pasqual (Padova) are thanked for ICP-MS and XRF analysis. Field assistance by K. Pande, C.J. Sprain, I.M. Fendley, T. Mittal, M.R. Richards and A.J. Tholt is appreciated. We thank Leone Melluso very much for lively and stimulating discussions on the Deccan. This work greatly benefitted from detailed and constructive reviews by W. Bohrson, R. Trumbull and three anonymous reviewers.

Supplementary materials

Supplementary material associated with this article can be found, in the online version, at doi:10.1016/j.epsl.2026.119847.

Data availability

Data will be made available on request.

References

Allègre, C.J., Birck, J.L., Capmas, F., Courtillot, V., 1999. Age of the Deccan traps using 187Re–187Os systematics. Earth Planet. Sci. Lett. 170, 197–204. https://doi.org/10.1016/S0012-821X(99)00110-7.

Annen, C., Blundy, J.D., Sparks, R.S.J., 2006. The genesis of intermediate and silicic magmas in deep crustal hot zones. J. Petrol. 47, 505–539. https://doi.org/10.1093/petrology/egi084.

Aulbach, S., Mungall, J.E., Pearson, D.G., 2016. Distribution and processing of highly siderophile elements in cratonic mantle lithosphere. Rev. Mineral. Geochem. 81, 239–304. https://doi.org/10.2138/rmg.2016.81.5.

Basu, A.R., Saha-Yannopoulos, A., Chakrabarty, P., 2020. Lithos A precise geochemical volcano-stratigraphy of the Deccan traps. Lithos 376–377, 105754. https://doi.org/10.1016/j.lithos.2020.105754.

Beane, J.E., Turner, C.A., Hooper, P.R., Subbarao, K.V., Walsh, J.N., 1986. Stratigraphy, composition and form of the Deccan Basalts, Western Ghats, India. Bull. Volcanol. 48, 61–83. https://doi.org/10.1007/BF01073513.

Bohrson, W.A., Spera, F.J., Heinonen, J.S., Brown, G.A., Scruggs, M.A., Adams, J.V., Takach, M.K., Zeff, G., Suikkanen, E., 2020. Diagnosing open-system magmatic processes using the Magma Chamber Simulator (MCS): part I–major elements and phase equilibria. Contrib. Mineral. Petrol. 175, 1–29.

Callegaro, S., Marzoli, A., Bertrand, H., Blichert-Toft, J., Reisberg, L., Cavazzini, G., Jourdan, F., Davies, J.H.F.L., Parisio, L., Bouchet, R., Paul, A., Schaltegger, U., Chiaradia, M., 2017. Geochemical constraints provided by the Freetown Layered Complex (Sierra Leone) on the origin of high-ti tholeiitic CAMP magmas. J. Petrol. 58, 1811–1840. https://doi.org/10.1093/petrology/egx073.

Callegaro, S., Baker, D.R., Renne, P.R., Melluso, L., Geraki, K., Whitehouse, M.J., De Min, A., Marzoli, A., 2023. Recurring volcanic winters during the latest Cretaceous: sulfur and fluorine budgets of Deccan Traps lavas. Sci. Adv. 9, eadg8284. https://doi.org/10.1126/sciadv.adg8284.

Capriolo, M., Callegaro, S., Deegan, F.M., Merle, R., Jeon, H., Whitehouse, M.J., Aradi, L. E., Storm, M., Renne, P.R., Baker, D.R., Dal Corso, J., Newton, R.J., Szabó, C., Carvalho, B.B., Youbi, N., Marzoli, A., 2024. Dynamic evolution of the transcrustal plumbing system in large igneous provinces: geochemical and microstructural insights from glomerocrysts and melt inclusions. J. Petrol. 65, egae103. https://doi.org/10.1093/petrology/egae103.

Carlson, R.W., 2005. Application of the Pt–Re–Os isotopic systems to mantle geochemistry and geochronology. Lithos 82, 249–272. https://doi.org/10.1016/j.lithos.2004.08.003.

Cashman, K.V., Sparks, R.S.J., Blundy, J.D., 2017. Vertically extensive and unstable magmatic systems: a unified view of igneous processes. Science 355, 6331. https://doi.org/10.1126/science.aag3055.

Chatterjee, N., 2024. Petrogenesis of the Deccan high-Mg basalts and picrites. Contrib. Mineral. Petrol. 179, 90. https://doi.org/10.1007/s00410-024-02172-7.

Chiaradia, M., Müntener, O., Beate, B., 2020. Effects of aseismic ridge subduction on the geochemistry of frontal arc magmas. Earth Planet. Sci. Lett. 531, 115984. https://doi.org/10.1016/j.epsl.2019.115984.

Cox, K.G., Hawkesworth, C.J., 1985. Geochemical stratigraphy of the Deccan Traps at Mahabaleshwar, Western Ghats, India, with implications for open system magmatic processes. J. Petrol. 26, 355–377. https://doi.org/10.1093/petrology/26.2.355.

Creaser, R.A., Papanastassiou, D.A., Wasserburg, G.J., 1991. Negative thermal ion mass spectrometry of osmium, rhenium and iridium. Geochim. Cosmochim. Acta 55, 397–401. https://doi.org/10.1016/0016-7037(91)90427-7.

Cucciniello, C., Langone, A., Melluso, L., Morra, V., Mahoney, J.J., Meisel, T., Tiepolo, M., 2010. U-Pb Ages, Pb-Os isotope ratios, and platinum-group element (PGE) composition of the West-Central Madagascar flood basalt province. J. Geol. 118, 523–541.

Day, J.M.D., Woodland, S.J., Nutt, K.L., Stroncik, N., Larsen, L.M., Trumbull, R.B., Pearson, D.G., 2024. Highly siderophile element evidence for mantle plume involvement during opening of the Atlantic Ocean. Earth Planet. Sci. Lett. 641, 118768. https://doi.org/10.1016/j.epsl.2024.118768.

Fendley, I.M., Mittal, T., Sprain, C.J., Marvin-DiPasquale, M., Tobin, T.S., Renne, P.R., 2019. Constraints on the volume and rate of Deccan Traps flood basalt eruptions using a combination of high-resolution terrestrial mercury records and geochemical box models. Earth Planet. Sci. Lett. 524, 115721. https://doi.org/10.1016/j.epsl.2019.115721.

Gannoun, A., Burton, K.W., Day, J.M.D., Harvey, J., Schiano, P., Parkinson, I., 2016. Highly siderophile element and Os isotope systematics of volcanic rocks at divergent and convergent plate boundaries and in intraplate settings. Rev. Mineral. Geochem. 81, 651–724. https://doi.org/10.2138/rmg.2016.81.11.

Haase, K.M., Regelous, M., Schöbel, S., Günther, T., de Wall, H., 2019. Variation of melting processes and magma sources of the early Deccan flood basalts, Malwa Plateau, India. Earth Planet. Sci. Lett. 524, 115711. https://doi.org/10.1016/j.epsl.2019.115711.

Halfar, M.C., Peters, B.J., Day, J.M.D., Schönbächler, M., 2023. An isotopically enriched mantle component in the source of Rodrigues, Réunion volcanic hotspot. Geochim. Cosmochim. Acta 355, 32–47. https://doi.org/10.1016/j.gca.2023.06.030.

Hart, S.R., 1984. A large-scale isotope anomaly in the Southern Hemisphere mantle. Nature 309, 753–757. https://doi.org/10.1038/309753a0.

Hart, S.R., Gaetani, G.A., 2006. Mantle Pb paradoxes: the sulfide solution. Contrib. Mineral. Petrol. 152, 295–308. https://doi.org/10.1007/s00410-006-0108-1.
Harvey, J., Dale, C.W., Gannoun, A., Burton, K.W., 2011. Osmium mass balance in peridotite and the effects of mantle-derived sulphides on basalt petrogenesis. Geochim. Cosmochim. Acta 75, 5574–5596. https://doi.org/10.1016/j.gca.2011.07.001.
Harvey, J., Warren, J.M., Shirey, S.B., 2016. Mantle sulfides and their role in Re–Os and Pb isotope geochronology. Rev. Mineral. Geochem. 81, 579–649. https://doi.org/10.2138/rmg.2016.81.10.
Heinonen, J.S., Carlson, R.W., Riley, T.R., Luttinen, A.V., Horan, M.F., 2014. Subduction-modified oceanic crust mixed with a depleted mantle reservoir in the sources of the Karoo continental flood basalt province. Earth Planet. Sci. Lett. 394, 229–241. https://doi.org/10.1016/j.epsl.2014.03.012.
Hoyer, P.A., Haase, K.M., Regelous, M., Fluteau, F., 2023. Systematic and temporal geochemical changes in the upper Deccan Lavas: implications for the magma plumbing system of flood basalt provinces. Geochem. Geophys. Geosyst. 24, 1–20. https://doi.org/10.1029/2022GC010750.
Janney, P.E., Shirey, S.B., Carlson, R.W., Pearson, D.G., Bell, D.R., Le Roex, A.P., Ishikawa, A., Nixon, P.H., Boyd, F.R., 2010. Age, composition and thermal characteristics of South African off-craton mantle lithosphere: evidence for a multi-stage history. J. Petrol. 51, 1849–1890. https://doi.org/10.1093/petrology/egq041.
Kale, V.S., Dole, G., Shandilya, P., Pande, K., 2019. Stratigraphy and correlations in Deccan Volcanic Province, India: quo vadis? GSA Bull. 132, 588–607. https://doi.org/10.1130/B35018.1.
Kasbohm, J., Schoene, B., 2018. Rapid eruption of the Columbia River flood basalt and correlation with the mid-Miocene climate optimum. Sci. Adv. 4, eaat8223. https://doi.org/10.1126/sciadv.aat8223.
Karakas, O., Dufek, J., 2015. Melt evolution and residence in extending crust: thermal modeling of the crust and crustal magmas. Earth Planet. Sci. Lett. 425, 131–144. https://doi.org/10.1016/j.epsl.2015.06.001.
Kent, D.V., Olsen, P.E., Wang, H., Schaller, M.F., Et-Touhami, M., 2024. Correlation of sub-centennial-scale pulses of initial Central Atlantic Magmatic Province lavas and the end-Triassic extinctions. Proc. Natl. Acad. Sci. USA 121, e2415486121. https://doi.org/10.1073/pnas.2415486121.
Mahoney, J., Macdougall, J.D., Lugmair, G.W., Murali, A.V., Das, M.S., Gopalan, I.S., 1982. Origin of the Deccan Trap flows at Mahabaleshwar inferred from Nd and Sr isotopic and chemical evidence. Earth Planet. Sci. Lett. 60, 47–60.
Mahoney, J.J., MacDougall, J.D., Lugmair, G.W., Murali, A.V., Sankar Das, M., Gopalan, K., 2000. Geochemistry of flood basalts of the toranmal section, Northern Deccan Traps, India: implications for regional deccan stratigraphy. J. Petrol. 41, 1099–1120. https://doi.org/10.1093/petrology/41.7.1099.
Marzoli, A., Renne, P.R., Andreasen, R., Spiess, R., Chiaradia, M., Ruth, D.C.S., Tholt, A. J., Pande, K., Costa, F., 2022. The shallow magmatic plumbing system of the Deccan Traps, evidence from plagioclase megacrysts and their host Lavas. J. Petrol. 63, 1–32. https://doi.org/10.1093/petrology/egac075.
McDonough, W.F., Sun, S.S., 1995. The composition of the Earth. Chem. Geol. 120, 223–253. https://doi.org/10.1016/0009-2541(94)00140-4.
Meisel, T., Walker, R.J., Irving, A.J., Lorand, J.P., 2001. Osmium isotopic compositions of mantle xenoliths: a global perspective. Geochim. Cosmochim. Acta 65, 1311–1323. https://doi.org/10.1016/S0016-7037(00)00566-4.
Melluso, L., Sethna, S.F., D'Antonio, M., Javeri, P., Bennio, L., 2002. Geochemistry and petrogenesis of sodic and potassic mafic alkaline rocks in the Deccan Volcanic Province, Mumbai Area (India). Mineral. Petrol. 74, 323–342. https://doi.org/10.1007/s007100200009.
Melluso, L., Mahoney, J.J., Dallai, L., 2006. Mantle sources and crustal input as recorded in high-Mg Deccan Traps basalts of Gujarat (India). Lithos 89, 259–274. https://doi.org/10.1016/j.lithos.2005.12.007.
Meyzen, C.M., Cedex, L., Ludden, J.N., Humler, E., Storey, M., 2005. New insights into the origin and distribution of the DUPAL isotope anomaly in the Indian Ocean mantle from MORB of the Southwest Indian Ridge. Geochem. Geophys. Geosyst. 6, Q11K11. https://doi.org/10.1029/2005GC000979.
Mittal, T., Richards, M.A., Fendley, I.M., 2021. The magmatic architecture of continental flood basalts I: observations from the Deccan Traps. J. Geophys. Res. Solid Earth 126, 1–54. https://doi.org/10.1029/2021JB021808.
Moore, N.E., Grunder, A.L., Bohrson, W.A., Carlson, R.W., Bindeman, I.N., 2020. Changing mantle sources and the effects of crustal passage on the Steens Basalt, SE Oregon: chemical and isotopic constraints. Geochem. Geophys. Geosyst. 21, e2020GC008910. https://doi.org/10.1029/2020GC008910.
Morgan, W.J., 1972. Plate motions and deep mantle convection. In: Studies in Earth and Space Sciences, 132. The Geological Society of America Memoir, pp. 7–22. https://doi.org/10.1130/MEM132-p7. R. Shagam, R. B. Hargraves, W. J. Morgan, F. B. Van Houten, C. A. Burk, H. D. Holland, L. C. Hollister.
Pakulla, J.J., Jansen, M.W., Duraiswami, R.A., Gadpallu, P., Tusch, J., Jentzsch, C., Braukmüller, N., Wombacher, F., Münker, C., 2023. Trace element and Sr-Nd-Hf-Pb isotope evidence for a multi-magma chamber system beneath the Deccan Volcanic Province, India. Chem. Geol. 640, 121749. https://doi.org/10.1016/j.chemgeo.2023.121749.
Peng, Z.X., Mahoney, J., Hooper, P., Harris, C., Beane, J., 1994. A role for lower continental crust in flood basalt genesis? Isotopic and incompatible element study of the lower six formations of the western Deccan Traps. Geochim. Cosmochim. Acta 58, 267–288. https://doi.org/10.1016/0016-7037(94)90464-2.
Peters, B.J., Day, J.M.D., Taylor, L.A., 2016. Early mantle heterogeneities in the Réunion hotspot source inferred from highly siderophile elements in cumulate xenoliths. Earth Planet. Sci. Lett. 448, 150–160. https://doi.org/10.1016/j.epsl.2016.05.015.
Peters, B.J., Day, J.M.D., 2017. A geochemical link between plume head and tail volcanism. Geochem. Perspect. Lett. 5, 29–34. https://doi.org/10.7185/geochemlet.1742.
Peters, B.J., Day, J.M.D., Greenwood, R.C., Hilton, D.R., Gibson, J., Franchi, I.A., 2017. Helium–oxygen–osmium isotopic and elemental constraints on the mantle sources of the Deccan Traps. Earth Planet. Sci. Lett. 478, 245–257. https://doi.org/10.1016/j.epsl.2017.08.042.
Peucker-Ehrenbrink, B., Jahn, B.M., 2001. Rhenium-osmium isotope systematics and platinum group element concentrations: loess and the upper continental crust. Geochem. Geophys. Geosyst. 2, 1061. https://doi.org/10.1029/2001GC000172.
Reisberg, L., Aulbach, S., 2025. Continental lithospheric mantle. In: Weis, D., Anbar, A. (Eds.), Treatise on Geochemistry, Treatise on Geochemistry, 3rd ed., 1. Elsevier, UK, pp. 773–865. https://doi.org/10.1016/B978-0-323-99762-1.00079-6. dx.
Rocha-Junior, E.R.V., Puchtel, I.S., Marques, L.S., Walker, R.J., Machado, F.B., Nardy, A. J.R., Babinski, M., Figueiredo, A.M.G., 2012. Re-Os isotope and highly siderophile element systematics of the Paraná continental flood basalt system. Earth Planet. Sci. Lett. 337-338, 164–173.
Rudnick, R.L., Gao, S., 2014. Composition of the continental crust. In: Holland, H.D., Turekian, K.K. (Eds.), Treatise on Geochemistry. Elsevier, UK (Oxford), pp. 1–64, 3.
Saal, A.E., Rudnick, R.L., Ravizza, G.E., Hart, S.R., 1998. Re–Os isotope evidence for the composition, formation and age of the lower continental crust. Nature 393, 58–61. https://doi.org/10.1038/29966.
Santosh, M., He, X.F., Waterton, P., Szilas, K., Pearson, D.G., 2020. Chromitites from an Archean layered intrusion in the Western Dharwar Craton, southern India. Lithos 376–377, 105772. https://doi.org/10.1016/j.lithos.2020.105772.
Schiano, P., David, K., Vlastélic, I., Gannoun, A., Klein, M., Nauret, F., Bonnand, P., 2012. Osmium isotope systematics of historical lavas from Piton de la Fournaise (Réunion Island, Indian Ocean). Contrib. Mineral. Petrol. 164, 805–820. https://doi.org/10.1007/s00410-012-0774-0.
Schoene, B., Eddy, M.P., Samperton, K.M., Keller, C.B., Keller, G., Adatte, T., Khadri, S.F. R., 2019. U-Pb constraints on pulsed eruption of the Deccan Traps across the end-Cretaceous mass extinction. Science 363, 862–866. https://doi.org/10.1126/science.aau2422.
Self, S., Mittal, T., Dole, G., Vanderkluysen, L., 2022. Toward understanding Deccan volcanism. Annu. Rev. Earth Planet. Sci. 50, 477–506. https://doi.org/10.1146/annurev-earth-012721-051416.
Sheth, H.C., 2007. Plume-related regional pre-volcanic uplift in the Deccan Traps: absence of evidence, evidence of absence. Foulger, G.R., and Jurdy, D.M., eds., Plates, Plumes, and Planetary Processes Geol. Soc. Am. Spec. Pap. 430, 785–813. https://doi.org/10.1130/2007.2430(36).
Simonetti, A., Goldstein, S.L., Schmidberger, S.S., Viladkar, S.G., 1998. Geochemical and Nd, Pb, and Sr isotope data from Deccan alkaline complexes–inferences for mantle sources and plume–lithosphere interaction. J. Petrol. 39, 1847–1864. https://doi.org/10.1093/petroj/39.11-12.1847.
Spera, F.J., Bohrson, W.A., 2001. Energy-constrained open-system magmatic processes I: general model and energy-constrained assimilation and fractional crystallization (EC-AFC) formulation. J. Petrol. 42 (5), 999–1018. https://doi.org/10.1093/petrology/42.5.999.
Sprain, C., Renne, P., Clemens, W., Wilson Mantilla, G., 2018. Calibration of chron C29r: New high-precision geochronologic and paleomagnetic constraints from the HellCreek region, Montana. GSA Bull. 130, 1615–1644. https://doi.org/10.1130/B31890.1.
Sprain, C.J., Renne, P.R., Vanderkluysen, L., Pande, K., Self, S., Mittal, T., 2019. The eruptive tempo of Deccan volcanism in relation to the Cretaceous-Paleogene boundary. Science 363, 866–870. https://doi.org/10.1126/science.aav1446.
Tegner, C., Wilson, J.R., Robins, B., 2005. Crustal assimilation in basalt and jotunite: constraints from layered intrusions. Lithos 83, 299–316. https://doi.org/10.1016/j.lithos.2005.03.007.
Tholt, A.J., Renne, P.R., Marzoli, A., Vanderkluysen, L., Mohabey, D., Samant, B., Dhobale, A., Pande, K., Self, S., 2023. Geochronological constraints on the evolution and petrogenesis of the Malwa Plateau subprovince of the Deccan Traps. Geochem. Geophys. Geosyst. 24, e2023GC011137. https://doi.org/10.1029/2023GC011137.
Vanderkluysen, L., Mahoney, J.J., Hooper, P.R., Sheth, H.C., Ray, R., 2011. The feeder system of the Deccan Traps (India): insights from dike geochemistry. J. Petrol. 52, 315–343. https://doi.org/10.1093/petrology/egq082.
Völkening, J., Walczyk, T., Heumann, K.G., 1991. Osmium isotope ratio determinations by negative thermal ionization mass spectrometry. Int. J. Mass Spectrom. Ion Process. 105, 147–159. https://doi.org/10.1016/0168-1176(91)80077-Z.
Widdowson, M., Walsh, J.N., Subbarao, K.V., 1997. The geochemistry of Indian bole horizons: palaeoenvironmental implications of Deccan intravolcanic palaeosurfaces. In: Widdowson, M. (Ed.), Palaeosurfaces: Recognition, Reconstruction and Palaeoenvironmental Interpretation, Palaeosurfaces: Recognition, Reconstruction and Palaeoenvironmental Interpretation, 120. Geological Society Special Publications, pp. 269–281.
Zindler, A., Hart, S.R., 1986. Chemical geodynamics. Annu. Rev. Earth Planet. Sci. 14, 493–571.